Available online at www.sciencedirect.com
ScienceDirect
Journal of Non-Crystalline Solids 354 (2008) 2909–2913
JOURNAL OF NON-CRYSTALLINE SOLIDS
www.elsevier.com/locate/jnoncrysol

Electrical conductivity and Meyer–Neldel rule: The role of localized states in hydrogenated amorphous silicon

T.A. Abtew [a,b], MingLiang Zhang [a], Yue Pan [a], D.A. Drabold [a,*]

[a] Department of Physics and Astronomy, Ohio University, Athens, Ohio 45701-2979, USA
[b] Department of Physics, Center for High Performance Simulation, North Carolina State University, Raleigh, NC 27695, USA

Available online 12 February 2008

Abstract

The Meyer–Neldel rule (MNR) has been observed in recent calculations of the electrical conductivity of hydrogenated amorphous silicon. To elucidate the origin of this effect, we have performed comparative studies on crystalline Si and non-hydrogenated a-Si. We find that the MNR is not present in the crystal, and is present in a-Si. This suggests that the existence of localized states and the energy dependence of the electron-lattice coupling for these states is an essential feature of the MNR for amorphous phases of silicon.

PACS: 71.23.−k; 71.23.An; 72.15.Cz

Keywords: Silicon; Conductivity

1. Introduction

In a wide temperature (T) range, the dependence of the DC conductivity σ of a-Si, a-Si:H, and other disordered systems approximately follows the Arrhenius form

$$\sigma(T) = \sigma_0 \exp\left(-\frac{E_a}{k_B T}\right). \quad (1)$$

A plot of the logarithm of the pre-exponential factor $\ln \sigma_0$ against activation energy E_a is linear. This linearity has been named the Meyer–Neldel rule (MNR) [1], after its discoverers. It is observed in many materials, and its ubiquity provides a compelling challenge to workers in condensed matter theory [2,3]. Its occurrence in diverse systems seems to demand an explanation not specific to a-Si or a-Si:H.

In recent work [4], we studied the electrical conductivity of a-Si and a-Si:H, using a density functional code, the Kubo–Greenwood formula, and a process of thermal averaging for selected temperatures. Our calculations clearly exhibit the Meyer–Neldel rule for a-Si:H. The existence of the MNR in our simulations provides an opportunity to explore the origin of the MNR from an atomistic perspective, since we may extract detailed information about the electronic structure, lattice dynamics, transition matrix elements etc. This paper contributes to a body of work analyzing the MNR, and has the advantage that it is based on computer models of a-Si:H that capture aspects of the network disorder.

To clarify the origin of the MNR, we have used the same procedure to compute the conductivity of crystalline silicon (c-Si) and (unhydrogenated) a-Si. The results reveal no Meyer–Neldel rule for c-Si (e.g., a constant conductivity pre-exponential factor) and a clear MNR in a-Si. A primary difference between the crystalline and amorphous systems is that the latter possess localized, and 'unevenly extended' states. Since the coupling of the lattice to these states is strongly energy-dependent (deeper states, larger coupling) [5,6], we infer that the Meyer–Neldel compensation in this system is a joint consequence of (1) the existence of localized states, and (2) the energy-dependence of the electron–phonon coupling.

* Corresponding author.
E-mail address: drabold@ohio.edu (D.A. Drabold).

0022-3093/$ - see front matter © 2008 Elsevier B.V. All rights reserved.
doi:10.1016/j.jnoncrysol.2007.09.103

At the end of the paper, a heuristic analysis supporting this view is given following an idea developed in electron transfer and small polaron contexts [7,8].

2. Constraints on theory

As we discuss elsewhere [4], the conductivity may be computed using a standard density functional code SIESTA [9], and linear response theory (the Kubo–Greenwood formula [10]). The temperature dependence of the conductivity is obtained by thermally averaging the Kubo formula over suitable constant temperature simulations. Here, we compute the conductivity for a 64-atom diamond supercell. We have prepared these models for eight different temperatures between 200 K and 1000 K. Each model was equilibrated to the desired temperature for 5.0 ps. Once equilibrated, we performed constant temperature MD simulations for another 1000 steps to obtain an average DC conductivity for each temperature.

2.1. Conductivity of intrinsic c-Si

In Fig. 1 we report the DC conductivity of c-Si as a function of temperature for the intrinsic case. The conductivity changes from $0.5 \times 10^{-10}\ \Omega^{-1}\ \mathrm{cm}^{-1}$ for $T = 200$ K to $0.2 \times 10^{1}\ \Omega^{-1}\ \mathrm{cm}^{-1}$ for $T = 1000$ K. Increasing the temperature of the system increases the number of carriers (electrons in conduction band and holes in valence band) and therefore increases the conductivity. In the relaxation time approximation, the conductivity is written as

$$\sigma(T) \propto \frac{1}{a^3} e^{-E_a/k_B T}\left[\frac{e^2\tau}{m^*}\right], \tag{2}$$

where a is the lattice constant of Si, m^* is the effective mass of a carrier, E_a is the activation energy ($E_a = E_C - \mu$ or $E_a = \mu - E_V$, μ is chemical potential). The temperature dependence of the mean free time τ, due to scattering of carriers with phonons, decays with increasing temperature according to a power law for carriers in extended states. At $T = 300$ K, the observed conductivity is about $2.7 \times 10^{-6}\ \Omega^{-1}\ \mathrm{cm}^{-1}$ [11], the calculated value is about $10^{-6}\ \Omega^{-1}\ \mathrm{cm}^{-1}$, the same order of magnitude. By dividing the DC conductivity into two regions of low temperature ($T < 500$ K) and high temperature ($T > 500$ K) we extracted E_a and σ_0 in Eq. (1). For low T, we have obtained $E_a \sim 0.48$ eV and $\sigma_0 \sim 64\ \Omega^{-1}\ \mathrm{cm}^{-1}$. For high T, $E_a \sim 0.62$ eV and $\sigma_0 \sim 2.3 \times 10^3\ \Omega^{-1}\ \mathrm{cm}^{-1}$.

2.2. Conductivity in doped c-Si

The Fermi level shifts with doping and temperature change [12,13]. In our work, we simulate doping by simply shifting the Fermi level. This procedure allows us to 'scan' the optical gap and compute conductivity for different doping (both n-type and p-type). Our scheme is quite different from an experiment. For example, it is known that the energy of defect states depends upon the location of the Fermi level and the density [14], so that a proper calculation of doping (meaning with explicit substitution of the donor or acceptor species) should be carried out self-consistently. Our procedure is thus highly idealized. Therefore, in this approach, it is not easy to correlate the conductivities we predict for a specific Fermi level position with the experimental concentration of dopant atoms. The computed DC conductivity for different temperatures as a function of chemical potential is shown in Fig. 2.

2.3. Absence of Meyer–Neldel rule in c-Si

By plotting σ as a function of $1/T$ for various doping (that is, various shifted Fermi levels), we extracted σ_0 and E_a for c-Si for two different temperature regimes.

An ideal Meyer–Neldel dependence would yield

$$\ln \sigma_0 = \ln \sigma_{00} + E_a/E_{MN}, \tag{3}$$

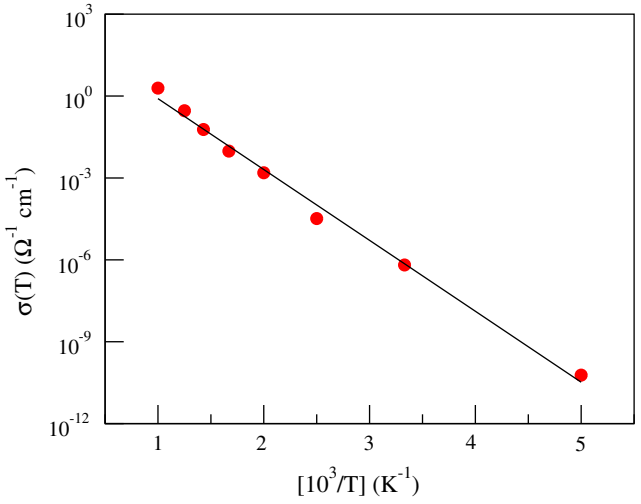

Fig. 1. DC conductivity of intrinsic c-Si obtained by averaging over 1000 configurations, agree with experimental values [11].

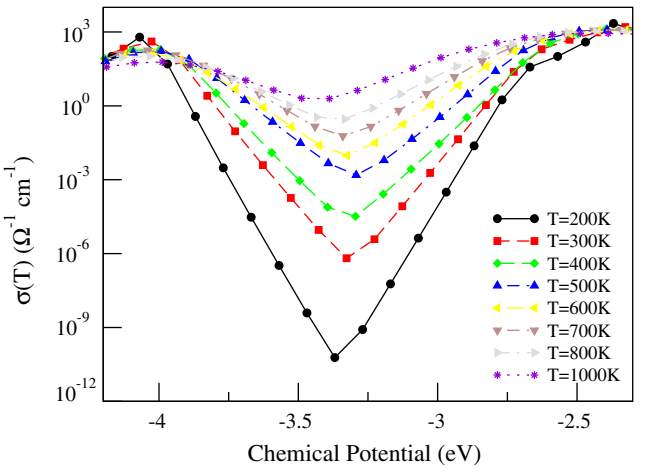

Fig. 2. DC conductivity of c-Si (the middle of the gap lies near chemical potential $\mu = -3.38$ eV) as a function of doping.

with slope $1/E_{MN}$ in $\ln\sigma_0$ vs. E_a plot. For 200 K < T < 500 K, $\ln\sigma_0$ vs. E_a is shown in Fig. 3, and for 500 K < T < 1000 K in Fig. 4. The slope in Fig. 3 is small and negative while small and positive in Fig. 4. The magnitude of the slope is far smaller than what we observed for a-Si:H [4].

In crystalline samples, the activation energy $E_C-\mu$ or $\mu-E_V$ decreases with doping. With increasing doping, the effective mass m^* decreases while the relaxation time τ increases, so that the pre-exponential factor $\sigma_0 = \frac{e^2}{m^*}\tau\frac{1}{a^3}$ increases with dopant concentration. Since larger dopant concentration means smaller activation energy E_a and larger pre-exponential factor σ_0, $\ln\sigma_0$ vs. E_a displays a negative slope in Fig. 3. At higher temperatures, a small positive slope implies that activation energy decreases with increasing temperature. Higher temperature causes the optical gap to shrink [11,15] for both crystalline and amorphous material. For this reason, we may conclude that crystalline models have an exceedingly weak MNR at higher temperature or do not exhibit the MNR at all, since MNR linearity is detected for a much broader temperature range in amorphous materials [3].

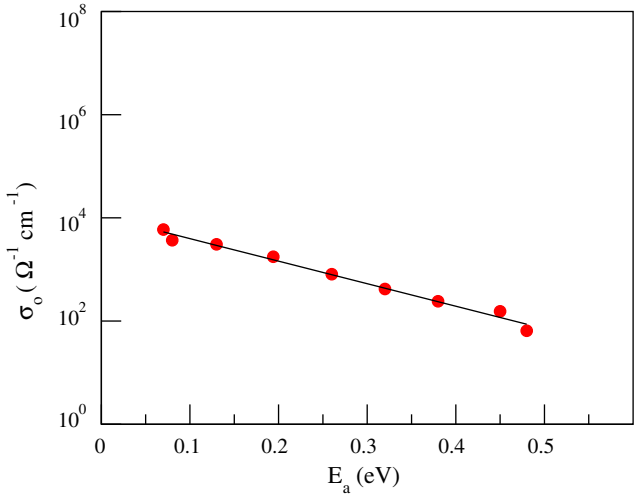

Fig. 3. The pre-exponential factor σ_0 as function of activation energy E_a for various doped c-Si samples for $T \leqslant 500$ K.

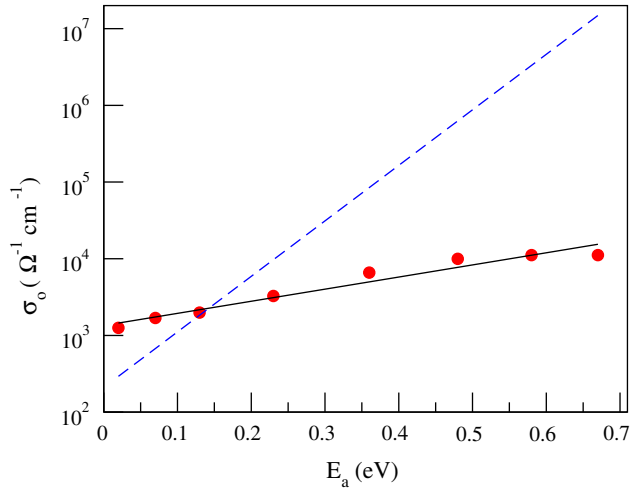

Fig. 4. The pre-exponential factor σ_0 as function of activation energy E_a for various doped c-Si samplesfor $T \geqslant 500$ K. The result for a-Si:H is shown in dashed line.

2.4. Meyer–Neldel rule in non-hydrogenated material

Both experiments [3] and simulation [4] show that Meyer–Neldel rule exists in various a-Si:H ($\mu = -3.80$ eV for pure sample) samples with $E_{MN} \approx 0.06$ eV. A comparison with non-hydrogenated samples a-Si ($\mu = -3.48$ eV for pure sample) will be helpful to infer the origin of MNR. From previous σ vs. $1/T$ data of a 64-atom a-Si model, (cf. Fig. 3 of Ref. [4]) we extract σ_0 and E_a, and determine that $E_{MN} = 0.11$ eV.

3. Discussion

There are two T-dependent factors that affect the DC conductivity of an amorphous semiconductor, such as a-Si and a-Si:H: (a) the effective number of carriers, (b) the mean velocity obtained by carriers under the influence of field and scattering. In an ideal model with no mid-gap states, the number of holes is $n_h \propto e^{-(\mu-E_V)/kT}$. $(\mu - E_V)$ and $(E_C - \mu)$, activation energies for holes and electrons respectively, are fairly insensitive to T (see Figs. 3 and 4 of Ref. [4]).

In a-Si:H and a-Si three conduction mechanisms exist: (i) carrier hopping from one localized state to an empty localized state; (ii) carrier hopping from a localized to an available extended state; (iii) carriers scattered from one extended state to another empty extended state. The assistance from phonons is indispensable for processes (i) and (ii). Because the tail states and mid-gap states are close to chemical potential, transition (i) are important in low temperature. Transition (ii) eventually plays a role in a moderate temperature. (iii) becomes meaningful only in higher temperature.

In the Kubo–Greenwood formula [3,4], the mean carrier velocity is determined by the transition matrix element. For transition from one localized state $|i\rangle$ with energy E_i to an empty localized state $|f\rangle$ with energy E_f, i.e. mechanism (i), the activation energy $E_a(T)$ may be written as [7,8]

$$E_a(T) = \frac{\lambda_{10}}{4}\left[1 + \frac{(E_f - E_i)}{\lambda_{10}}\right]^2, \tag{4}$$

λ_{10} is the reorganization energy of a-Si:H random network for carrier hopping,

$$\lambda_{10} = \frac{(e/2)^2}{4\pi\varepsilon_0}\left[\frac{1}{2\xi_f} + \frac{1}{2\xi_i} - \frac{1}{R}\right]\left[\frac{1}{\varepsilon_{op}} - \frac{1}{\varepsilon_s}\right], \tag{5}$$

ξ_f and ξ_i are localization radii for two localized states $|f\rangle$ and $|i\rangle$, R is the distance between two localization centers [7,8]. The two square brackets in Eq. (5) decrease with increasing temperature. The optical dielectric constant ε_{op}

is determined mainly by the number of carriers, the latter increases with temperature, so does ε_{op}. The static dielectric function ε_s, mainly from the random network, decreases with thermal vibration, therefore decreases with temperature. Thus the second bracket in Eq. (5) decreases with temperature. We have shown that the inverse participation ratio (IPR) as a function of (T) decreases (cf. Figs. 1 and 4 of Ref. [4]), so that localization length $\xi(T) = \frac{a}{[IPR(T)]^{1/3}}$ increases with temperature. The first bracket in (5) decreases with temperature.

The activation energy for transition (ii) depends on the height of escape barrier for localized carrier and available extended states and decreases with temperature. Thus for hopping dominant temperature range, i.e. mechanisms (i) and (ii), $E_a(T)$ decreases with temperature, though the dependence may be complicated. However to zeroth-order,

$$E_a(T) = E_a\left(1 - \frac{T}{T_m}\right), \tag{6}$$

activation energy decreases with temperature linearly. Substituting Eq. (6) into an Arrhenius type expression

$$\sigma(T) = \sigma_{00}\exp\left\{-\frac{E_a(T)}{k_B T}\right\}, \tag{7}$$

yields Eq. (3),

$$\begin{aligned}\sigma(T) &= \sigma_{00}\exp\left\{\frac{E_a}{k_B T_m} - \frac{E_a}{k_B T}\right\} \\ &= \sigma_{00}\exp\left\{\frac{E_a}{k_B T_m}\right\}\exp\left\{-\frac{E_a}{k_B T}\right\},\end{aligned} \tag{8}$$

with the identification $E_{MN} = k_B T_m$ and $\sigma_0 = \sigma_{00}\exp\left\{\frac{E_a}{k_B T_m}\right\}$, the Meyer–Neldel rule.

The decrease of activation energy with temperature, is an example of the more general idea of multi-excitation entropy [2], if we identify $E_a(T)$ as activation free energy G, E_a as the activation enthalpy, $\frac{E_a}{T_m}$ as the multi-excitation entropy S. At the same time, we notice that it is the localized states whose transition has an activation energy decreasing with temperature.

Accumulating enough phonons to assist a carrier to overcome a barrier (4) can be achieved in many different ways. The larger the activation energy, the more combinations of phonons the carrier and network may choose. Thus our picture seems compatible with the multi-excitation entropy picture [2]. It has been shown that the localized states at band edges strongly couple to the lattice [5,6], and for well-localized states, the electron-lattice coupling is directly proportional to the localization of the electron state as gauged by IPR. Therefore, the deeper the state (the higher the activation energy), the larger the impact of phonons on the carrier. The role of electron–phonon coupling is then three fold: (1) it supplies the energy to activate a localized carrier: for a process in which n phonons are absorbed, the probability is proportional to g^{2n}, g is the electron–phonon coupling constant; (2) The dependence of σ_0 on g is roughly a bell shape curve. For weak electron–phonon coupling, $\sigma_0 \propto g$, for strong coupling, $\sigma_0 \propto g^{-1}$ [16]. (3) the electron–phonon coupling enhances the static dielectric constant ε_s and therefore increases reorganization energy λ_{10}.

For an activated process described by Eq. (7), σ_{00} is the microscopic transition frequency (the Landau–Zener rate) and is determined by the nature of localized electronic states. Doping changes the number of carriers, and does not modify the tail states too much (not at all in our approximation). σ_{00} remains nearly constant. T_m in Eq. (6) measures how quickly the activation energy decreases with temperature, and is the temperature at which the activation disappears in a class of material. T_m is a quantity universal for a specific class of material. For a-Si:H, $E_{MN} = 0.065$ eV, about one half of the melting temperature of c-Si.

The hydrogen glass model [17] assumes that above the glass transition temperature T_g for H, the Fermi level is pinned between defect states and band tail states. Experimentally, a kink appears in the ln sigma vs. $1/T$ plot. Below T_g, the Fermi level moves upward for n-type material with decreasing T. This statistical shift of Fermi level effectively lowers the prefactor and in this model leads to MNR. The Meyer–Neldel rule exists in various disordered system, a-Si, a-Si:H, chalcogenide materials and even polymers. It is attractive to conjecture a common physical mechanism for these materials. Evidently, while the H glass model is a possible explanation for the case of a-Si:H, it is not relevant for all the different materials.

In conclusion, the calculations of conductivity for doped crystalline silicon samples show the absence of Meyer–Neldel rule in crystal samples. In a-Si and a-Si:H samples, due to the appearance of localized states, the activation energy for processes (i) and (ii) decreases with temperature. Meyer–Neldel rule emerges as a consequence of localized states.

Acknowledgements

DAD thanks Professor J. David Cohen (U. Oregon) for the first conjecture of the potential compensation effects of the energy-dependent electron-lattice coupling. We thank Professor Thomas Jackson (Penn. State U.) for helpful conversations, and indeed for urging us to undertake the calculations presented here. Research was sponsored by the US Army Research Office and US Army Research Laboratory and was accomplished under Cooperative Agreement Number W911NF-0-2-0026. The views and conclusions contained in this document are those of the authors and should not be interpreted as representing the official policies, either expressed or implied, of the Army Research Office, Army Research Laboratory, or the US Government. The US Government is authorized to reproduce and distribute reprints for Government purposes notwithstanding any copyright notation hereon. We also thank the National Science Foundation for support in

early phases of the work under Grants Nos. DMR 0600073 and 0605890.

References

[1] W. Meyer, H. Neldel, Z. Techn. Phys. 12 (1937) 588.
[2] A. Yelon, B. Movaghar, R.S. Crandall, Rept. Prog. Phys. 69 (2006) 1145.
[3] H. Overhof, P. Thomas, Electronic Transport in Hydrogenated Amorphous Silicon Springer Tracts in Modern Physics, vol. 114, Springer, Berlin, 1989.
[4] T. Abtew, M.-L. Zhang, D. Drabold, Phys. Rev. B 76 (2007) 045212.
[5] D.A. Drabold, P.A. Fedders, S. Klemm, O.F. Sankey, Phys. Rev. Lett. 67 (1991) 2179.
[6] R. Atta-Fynn, P. Biswas, D.A. Drabold, Phys. Rev. B 69 (2004) 245204.
[7] R.A. Marcus, Rev. Mod. Phys. 65 (1993) 599.
[8] G.D. Mahan, Many-Particle Physics, 1st Ed., Plenum, New York, 1981, p. 523;
H.G. Reik, in: J.T. Devereese (Ed.), Polarons in Ionic and Polar Semiconductors, North-Holland/American Elsevier, Amsterdam, 1972 (Chapter VII).
[9] J.M. Soler, E. Artacho, J.D. Gale, A. Garcia, J. Junquera, P. Ordejon, D. Sanchez-Portal, J. Phys. Condens. Matter 14 (2002) 2745.
[10] R. Kubo, J. Phys. Soc. Jpn. 12 (1957) 570;
D.A. Greenwood, Proc. Phys. Soc. 71 (1958) 585.
[11] C. Kittel, Introduction to Solid State Physics, 7th Ed., John Wiley, 1996;
K. Seeger, Semiconductor Physics: An Introduction, 4th Ed., Springer, Berlin, 1989.
[12] R.H. Williams, R.R. Varma, W.E. Spear, P.G. LeComber, J. Phys. C 12 (1979) L209.
[13] B. von Roedern, L. Ley, M. Cardona, Solid State Commun. 29 (1979) 415.
[14] See for example R.A. Street, Hydrogenated Amorphous Silicon, Cambridge University, Cambridge, 1991, p. 194.
[15] N.W. Ashcroft, N.D. Mermin, Solid State Physics, Brooks/Cole, Thomson, New York, 1976.
[16] H.A. Kramers, Physica 7 (1940) 284;
M.-L. Zhang, S.-S. Zhang, E. Pollak, J. Chem. Phys. 119 (2003) 11864.
[17] R.A. Street, Phys. Rev. Lett. 49 (1982) 1187;
R.A. Street, J. Kakalios, C.C. Tsai, T.M. Hayes, Phys. Rev. B35 (1987) 1316.